Radiotherapy and Oncology 201 (2024) 110571

Contents lists available at ScienceDirect

Radiotherapy and Oncology

journal homepage: www.thegreenjournal.com

Original Article

Guiding induction chemotherapy of locoregionally advanced nasopharyngeal carcinoma with ternary classification of predicted individual treatment effect

Zhiying Liang [a,1], Chao Luo [a,1], Shuqi Li [a,1], Yuliang Zhu [b,1], Wenjie Huang [a], Di Cao [a], Yifei Liu [a], Guangying Ruan [a], Shaobo Liang [c], Xi Chen [d], Kit-Ian Kou [e], Guoyi Zhang [f], Lizhi Liu [a,*], Haojiang Li [a,**]

[a] Department of Radiology, State Key Laboratory of Oncology in South China, Guangdong Key Laboratory of Nasopharyngeal Carcinoma Diagnosis and Therapy, Guangdong Provincial Clinical Research Center for Cancer, Sun Yat-sen University Cancer Center, Guangzhou 510060, China
[b] Nasopharyngeal Head and Neck Tumor Radiotherapy Department, Zhongshan City People's Hospital, Zhongshan 528400, China
[c] Department of Radiation Oncology, Third Affiliated Hospital of Sun Yat-sen University, Guangzhou 510630, China
[d] Department of Hepatobiliary Surgery, Sun Yat-Sen Memorial Hospital of Sun Yat-Sen University, Guangzhou 510120, China
[e] Department of Mathematics, Faculty of Science and Technology, University of Macau, Macao Special Administrative Region of China
[f] Department of Radiation Oncology, First People's Hospital of Foshan, Foshan 528000, China

ARTICLE INFO

Keywords:
Nasopharyngeal carcinoma
Induction chemotherapy
Overall survival
Treatment decision-making
Predicted individual treatment effect

ABSTRACT

Background and purpose: Induction chemotherapy (IC) before concurrent chemoradiotherapy does not universally improve long-term overall survival (OS) in locoregionally advanced nasopharyngeal carcinoma (LANPC). Conventional risk stratification often yields suboptimal IC decisions. Our study introduces a ternary classification of predicted individual treatment effect (PITE) to guide personalized IC decisions.

Materials and methods: A two-center retrospective analysis of 1,213 patients with LANPC was conducted to develop and validate prognostic models integrating magnetic resonance imaging and clinical data to estimate individual 5-year OS probabilities for IC and non-IC treatments. Differences in these probabilities defined PITE, facilitating patient stratification into three IC recommendation categories. Model effectiveness was validated using Kaplan–Meier estimators, decision curve-like analysis, and evaluations of variable importance and distribution.

Results: The models exhibited strong predictive performance in both treatments across training and cross-validation sets, enabling accurate PITE calculations and patient classification. Compared with non-IC treatment, IC markedly improved OS in the IC-preferred group (HR = 0.62, p = 0.02), had no effect in the IC-neutral group (HR = 1.00, p = 0.70), and worsened OS in the IC-opposed group (HR = 2.00, p = 0.03). The ternary PITE classification effectively identified 41.7 % of high-risk patients not benefiting from IC, and yielded a 2.68 % higher mean 5-year OS probability over risk-based decisions. Significantly increasing distributions of key prognostic indicators, such as metastatic lymph node number and plasma Epstein–Barr virus DNA level from IC-opposed to IC-preferred groups, further validated the clinical relevance of PITE classification.

Conclusion: The ternary PITE classification offers an accurate and clinically advantageous approach to guide personalized IC decision-making in patients with LANPC.

Abbreviation: CCRT, concurrent chemoradiotherapy; CI, confidence interval; C-index, concordance index; EBV, Epstein–Barr virus; HR, hazard ratio; IC, induction chemotherapy; LANPC, locoregionally advanced nasopharyngeal carcinoma; LASSO, least absolute shrinkage and selection operator; MRI, magnetic resonance imaging; NPC, nasopharyngeal carcinoma; OS, overall survival; PITE, predicted individual treatment effect.

* Corresponding author at: Department of Radiology, Sun Yat-sen University Cancer Center, Guangzhou 510060, China.
** Corresponding author at: Department of Radiology, Sun Yat-sen University Cancer Center, Guangzhou 510060, China.
E-mail addresses: liulizh@sysucc.org.cn (L. Liu), lihaoj@sysucc.org.cn (H. Li).
[1] These authors contributed equally to this work.

https://doi.org/10.1016/j.radonc.2024.110571
Received 5 May 2024; Received in revised form 26 September 2024; Accepted 3 October 2024
Available online 10 October 2024

Introduction

Nasopharyngeal carcinoma (NPC) is a head-and-neck cancer with strong etiological links to the Epstein–Barr virus (EBV) [1] and is highly prevalent in China [2]. Of the approximately 130,000 patients diagnosed with incident NPC annually worldwide [2], 80 % have locoregionally advanced NPC (LANPC) [3,4]. With treatment improvements, the 5-year overall survival (OS) rate for these patients is approximately 70–80 %; the survival rate is >90 % for those in an early-stage [5]. The cornerstone of LANPC treatment is concurrent chemoradiotherapy (CCRT) [6,7], and induction chemotherapy (IC) before CCRT is favored for its potential to improve survival rates [8,9] by addressing micrometastases. However, the heterogeneous nature of NPC [10] suggests that IC may not be universally beneficial, with some patients receiving no benefit or even experiencing harm. This variation in treatment effects underscores the need for an effective classification system to improve IC decisions.

The conventional IC decision-making in patients with LANPC has heavily depended on risk stratification [11,12], primarily using clinicopathologic and imaging-assessed factors, including tumor and nodal staging and the EBV-DNA level. Studies have tried to improve risk prediction accuracy by integrating more refined algorithms [13,14] and more comprehensive features from laboratory examinations [15,16], pathology [17], magnetic resonance imaging (MRI) [18,19], or positron emission tomography/computed tomography [13] radiomics signatures. High-risk individuals are considered suitable for optional IC [11,12,14]. Although useful, this methodology lacks precision for personalized medicine owing to its broad risk categories, which may oversimplify disease heterogeneity, causing suboptimal treatment decisions. The IC effect is a group-level average, expressed as the hazard ratio between treatment regimens with and without IC [20,21]. However, risk levels do not correlate directly with treatment benefits; individual patients with the same risk level may exhibit significant variations in characteristics and diverse responses to IC from the "average patient" [20]. Thus, the risk stratification approach is insufficient to guide individualized treatment strategies.

The predicted individual treatment effect (PITE) classification is an intuitive and direct approach for personalized treatment decisions [20,22]. The PITE causal framework utilizes predictive models to estimate individualized potential outcomes, including long-term OS probabilities, under different treatment regimens. The difference between these estimated prognoses represents the PITE. Despite its potential, the PITE approach has seldom been applied in NPC or other cancer studies. Thus, we aimed to personalize IC decision-making for patients with LANPC through a PITE-based classification to improve long-term survival.

Materials and methods

Study design and patients

This retrospective study was approved by the institutional ethics review board of Sun Yat-sen University Cancer Center (approval number: B2019-222-01) and performed in accordance with the Declaration of Helsinki. The requirement for informed consent was waived owing to the study's retrospective nature.

As described in the Fig. 1, patients newly diagnosed with NPC on pathology and treated with intensity-modulated radiotherapy at two tertiary hospitals were identified and selected. All patients were treated with intensity-modulated radiotherapy-based CCRT and optional IC, in accordance with the standardized treatment protocols [6,7]. Patients were followed up every 3 months during the first 2 years after diagnosis and biannually afterward. The study endpoint was OS, defined as the period from treatment initiation to death for any reason or last follow-up. The treatment regimens and protocols for NPC have been described [23] and are detailed in the Supplementary Methods.

MRI protocol and imaging assessment using a structured report template

Supplementary Methods detail the protocols for pretreatment MRI of the nasopharynx and neck. To ensure accuracy, two radiologists (L.L. and Y.L.) with >10 years of experience in NPC diagnosis assessed imaging features on MRI slices using a consensus process with a structured report template (Supplementary Tables S1 and S2) obtained previously [24], recording the extent of invasion of the primary lesion and surrounding structures and regional lymph nodes.

Establishment and validation of treatment-stratified prognostic models for OS

A detailed description of the collected patient characteristics is provided in the Supplementary Methods. Age, T-stage, N-stage, and pretreatment plasma EBV-DNA level were confirmed as clinical predictors and used to form a base model.

The patients were divided into the IC and non-IC groups based on their treatment regimens. A 1:1 random pair-matching method by balancing T- and N-stages was used to reduce clinician bias in treatment selection. The establishment process of the treatment-stratified prognostic models (IC and non-IC models) for OS was detailed in Fig. 2A. Both models were cross-validated using each other's training set as the

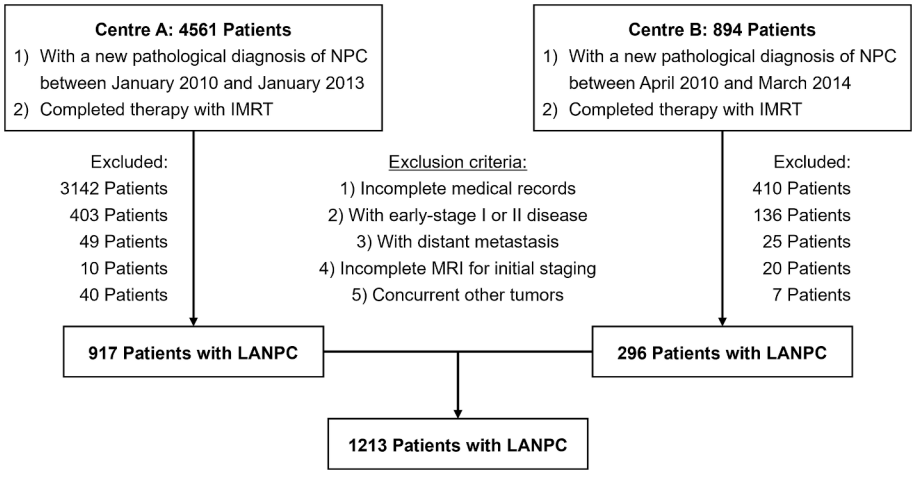

Fig. 1. Patient selection flowchart Abbreviations: NPC, nasopharyngeal carcinoma; IMRT, intensity-modulated radiotherapy; MRI, magnetic resonance imaging; LANPC, locoregionally advanced nasopharyngeal carcinoma.

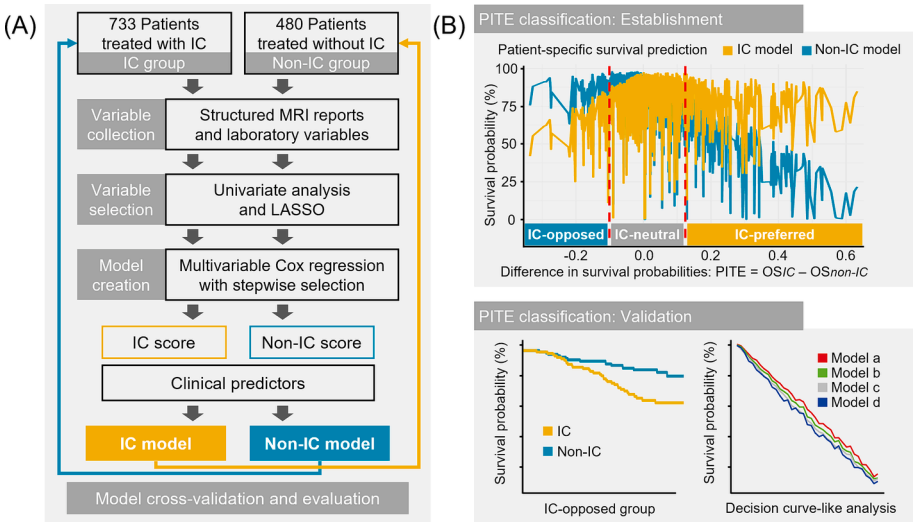

Fig. 2. Study workflow **(A)** Construction, cross-validation, and evaluation process of treatment-stratified prognostic models that can predict the long-term prognosis of patients who undergo IC or non-IC treatment regimens. For both IC and non-IC groups, univariate analysis and a LASSO analysis with five-fold cross-validation are conducted to select potential survival predictors from radiological and laboratory features. The comprehensive score is calculated by linearly combining algorithmically selected independent factors for OS and setting their Cox regression coefficients as weights. Treatment-stratified models (IC and non-IC models) are then developed based on the score and clinical predictors. (**B**) Establishment and validation of the three groups of PITE classification for treatment decision-making on IC. PITEs are calculated by the difference in the long-term survival probabilities based on the treatment-related prognostic models using the patient-specific survival prediction technique. Abbreviations: IC, induction chemotherapy; MRI, magnetic resonance imaging; LASSO, least absolute shrinkage and selection operator; PITE, predicted individual treatment effect; OS, overall survival.

validation set. The model performance for discrimination was evaluated using Harrell's concordance index (C-index), calibration using calibration curve analysis, and clinical net benefit using decision curve analysis.

Patient classification and validation of ternary PITE classification for IC decisions

The methodology for the survival prediction and ternary PITE classification is detailed in the Supplementary Methods. Using the IC and non-IC models, we calculated the 5-year OS probabilities and corresponding 95 % confidence intervals (CIs) for each patient through the patient-specific survival prediction technique [25] (Fig. 2B). Each patient was classified into one of the three PITE groups (IC-opposed, IC-neutral, and IC-preferred) based on the difference in the treatment-stratified OS probabilities and whether the corresponding CIs overlapped (Supplementary Figure S1). These groups represented patients with a reduced, comparable, or improved OS probability if treated with IC, respectively. Survival analyses were used to validate the ternary PITE classification in all patients and in pair-matched patients.

Comparing ternary PITE classification and conventional risk stratification for IC decisions

We compared the PITE classification with three conventional risk stratification methods for IC decision-making: EBV-DNA levels (1,000 copies/mL as cutoff for low- and high-risk [26]) and predicted mortality risks from the base and non-IC models (median risk score as cutoff for low- and high-risk). Risk-stratified survival analyses were conducted to identify high-risk patients potentially benefiting from IC treatment.

To assess the accuracy of identifying actual beneficiaries of IC treatment, survival analyses were conducted on patients who were in both the IC-preferred and high-risk groups and those exclusively categorized in the high-risk group. For a more direct comparison of clinical utility between PITE classification and conventional risk stratification, we conducted an updated decision curve-like analysis. This analysis utilized 1,000 bootstrap resampling to calculate the mean 5-year OS probabilities across various risk ratios and treatment strategies.

Supporting evidence for the PITE classification

A permutation method was employed to compute the relative importance of model-related variables. The distribution of variables within the PITE groups and distribution of PITE-classified patients within each T-stage, N-stage, and NPC extension pattern were examined. Furthermore, disparities in the adverse reaction incidence between PITE groups were analyzed.

Statistical analysis

The distribution differences of clinical characteristics were compared using Fisher's exact test or chi-squared test for categorical variables and Student's *t* test for continuous variables. The *U* test was used to compare the C-indices of the prognostic models. The Kaplan–Meier method with the log-rank test was used to compare survival differences between patients treated with and without IC. All statistical analyses were conducted in the open-source software R (version 4.0.1) using relevant packages (*stats*, *survival*, *Hmisc*, *glmnet*, *ggplot2*, *survminer*). A two-sided *p*-value <0.05 indicated statistical significance.

Results

Overall, 1,213 patients (924 men, 289 women) with a median (interquartile range) age of 46 (39−55) years were included. Among them, 733 and 480 patients were categorized to the IC and non-IC groups, respectively. The baseline characteristics of patients from each center and by treatment group are summarized in Supplementary Tables S3-S5. During a median follow-up of 59.5 (range: 3.4−91.0) months, 220/1213 (18.14 %) patients died, and the 5-year OS rate was 80.65 %. Altogether, 428 pairs were matched in the IC and non-IC groups (Supplementary Table S6).

The MRI structured report and laboratory features provided the basis for constructing prognostic models for predicting 5-year OS. Two treatment-specific comprehensive scores (IC and non-IC scores) for each patient were calculated based on the variables that remained after the selection process (Table 1). Then, two treatment-stratified prognostic models (IC and non-IC models, Table 1) based on the scores and clinical

Table 1
Multivariate Cox regression analysis of treatment-related prognostic models.

Variable	β[a]	HR (95 % CI)[a]	*p* value[a]
(1) IC model[b]			
IC score (linear predictor)[c]	1.05	2.85 (2.29–3.56)	<0.001
Invasion of musculus longus capitis	0.64	1.90 (1.28–2.84)	0.002
Invasion of infratemporal fossa	0.61	1.84 (1.04–3.26)	0.04
Invasion of jugular foramen	0.55	1.74 (1.05–2.87)	0.03
Bilateral retropharyngeal lymph node metastasis	0.39	1.47 (1.02–2.11)	0.04
Lymph node central necrosis	0.35	1.42 (1.00–2.01)	0.05
Number of metastatic lymph nodes	0.06	1.06 (1.03–2.21)	<0.001
Monocyte (10^9/L)			
<0.1		Reference	
0.1–0.6	0.41	1.50 (1.03–2.21)	0.04
≥0.6	−0.02	0.98 (0.14–7.10)	0.99
Albumin (g/L, continuous)	−0.03	0.97 (0.93–1.01)	0.12
Plasma EBV-DNA (10^3 copies/mL)			
<1		Reference	
<10	−0.02	0.98 (0.64–1.50)	0.93
≥10	−0.54	0.58 (0.37–0.92)	0.02
Age	0.03	1.03 (1.01–1.04)	<0.001
(2) Non-IC model[b]			
Non-IC score (linear predictor)[c]	0.96	2.62 (2.17–3.18)	<0.001
Slight skull base invasion[d]	−0.92	0.40 (0.19–0.85)	0.02
Invasion of carotid sheath	0.47	1.60 (1.00–2.56)	0.05
Invasion of jugular foramen	0.89	2.42 (1.10–5.34)	0.03
Invasion of orbit	1.10	2.99 (1.48–6.04)	0.002
Invasion of intracranial structures	0.86	2.35 (0.86–6.41)	0.09
Lymph node central necrosis	0.54	1.71 (1.03–2.84)	0.04
Number of metastatic lymph nodes	0.10	1.10 (1.06–1.15)	<0.001
Albumin (g/L)			
<40		Reference	
≥40	−0.94	0.39 (0.22–0.69)	0.001
Age	0.03	1.03 (1.01–1.04)	0.004

[a] Calculated by multivariate Cox regression.
[b] T-stage and N-stage are eliminated by stepwise selection.
[c] Calculated by stepwise multivariate Cox regression using features selected by LASSO (features are listed in the table).
[d] Pterygoid process and/or base of the sphenoid bone invasion only. Abbreviations: IC, induction chemotherapy; HR, hazard ratio; CI, confidence interval; EBV, Epstein − Barr virus.

predictors and a base model using clinical predictors alone were successfully constructed.

The prognostic model performance was evaluated. In the training sets, both IC and non-IC models outperformed the base model (C-indices, 0.789 vs. 0.740 and 0.721 vs. 0.660, respectively; both p <0.001; Table 2). In the validation sets, the C-index for OS prediction was significantly higher in the IC model than in the base model when applied to patients in the non-IC group (0.758 vs. 0.717, p <0.001); the non-IC model outperformed the base model for patients in the IC group (0.665 vs. 0.636, p = 0.03). Furthermore, calibration curves demonstrated robust agreement between predicted probabilities and actual observations in the validation sets for both IC and non-IC models (Supplementary Figure S2). The decision curve analysis in the validation set revealed that the IC and non-IC models provided greater clinical net benefits than the base model (Fig. 3A–B).

Both IC and non-IC models performed well and reliably predicted 5-year OS probabilities for both treatment regimens for each patient, facilitating patient classification into three PITE groups. Kaplan–Meier analysis (Fig. 3C–E) showed that, compared with non-IC treatment, IC was associated with improved OS probability in the IC-preferred group (hazard ratio [HR] = 0.62, 95 % CI = 0.41–0.93, p = 0.02); no significant change in the IC-neutral group (HR = 1.00, 95 % CI = 0.67–1.80, p = 0.70); and worse OS in the IC-opposed group (HR = 2.00, 95 % CI = 1.09–3.69, p = 0.03). This was additionally verified through Kaplan–Meier analysis in the pair-matched patients (p = 0.04, 0.59, and 0.001 in the IC-opposed, IC-neutral, and IC-preferred groups, respectively, Supplementary Figure S3A–C).

All three conventional risk stratification methods (non-IC model, base model, and EBV-DNA stratification) successfully differentiated between high-risk and low-risk groups; in high-risk patients identified by the base and non-IC models, IC treatment was potentially beneficial (Supplementary Figures S3D–F, S4, S5A–B). Given that the non-IC model outperformed the base model (Table 2), we used the PITE classification to further categorize high-risk patients identified by the non-IC model. Of these high-risk patients, 58.3 % (353/606) were also classified as IC-preferred. However, in the remaining 41.7 % (253/606) who were not identified as benefiting from IC by the PITE classification, there was no significant survival difference between IC and non-IC treatments (adjusted p = 0.005 and 0.72, respectively; Supplementary Figure S5C–D).

We further explored the characteristics between the IC-preferred and combined IC-neutral/opposed groups among these high-risk patients (Supplementary Table S7). The two groups had no significant differences in T-stage, N-stage, and clinical stage. Compared to the IC-preferred group, the combined IC-neutral/opposed group had a lower proportion of high plasma EBV-DNA level, lower hemoglobin levels, higher white blood cell and monocyte counts. In terms of radiological features, the combined IC-neutral/opposed group exhibited a higher proportion of mild/moderate soft-tissue involvement (palatine levator and longus capitis muscles) and slight skull base invasion, but a lower proportion of invasion of carotid sheath and T4 stage-related structures such as intracranial structures, orbit, superior and inferior orbital fissures.

The decision curve-like analysis further demonstrated the enhanced clinical utility of the ternary PITE classification over conventional risk stratification for IC decision-making. The OS curve for patients treated based on PITE classification was consistently higher than those for treatments based on clinical practice and all three risk stratification methods (Supplementary Figure S6, Fig. 3F). Specifically, PITE-based treatment exhibited a 4.83 % and 2.68 % higher mean 5-year OS probability compared to treatments according to clinical practice and non-IC model, respectively (Fig. 3F).

To increase validity of the ternary PITE classification, additional clinical evidence was sought. First, the five most influential factors for survival prediction were the number of metastatic lymph nodes, age, lymph node central necrosis, infratemporal fossa invasion, and plasma EBV-DNA level (Fig. 4A). Second, variable distributions were analyzed (Supplementary Table S8). The number of metastatic lymph nodes and plasma EBV-DNA level exhibited a significant ascending distribution from the IC-opposed to the IC-preferred groups (Fig. 4B). Furthermore, the proportion of patients classified as IC-preferred increased as the N-stage progressed from 1 to 4, or as the NPC extension pattern shifted from ascending (T3–4 N0–1) to mixed (T3–4 N2–3) and then to descending (T1–2 N2–3) (Fig. 4C). The proportion of patients classified

Table 2
Cross-validation and performance of treatment-related prognostic models and base model.

	Training set			Validation set		
Model	Patient group	C-index (95 % CI)	*p* value[a]	Patient group	C-index (95 % CI)	*p* value[a]
Non-IC model	Non-IC	0.789 (0.742–0.837)	<0.001	IC	0.665 (0.619–0.710)	0.03
Base model	Non-IC	0.740 (0.690–0.790)		IC	0.636 (0.589–0.682)	
IC model	IC	0.721 (0.677–0.765)	<0.001	Non-IC	0.758 (0.706–0.810)	<0.001
Base model	IC	0.660 (0.614–0.706)		Non-IC	0.717 (0.665–0.769)	

The base model is built based on the clinical predictors (age, T-stage, N-stage, and plasma EBV-DNA level). The models' discriminative ability is assessed using the C-index. The IC model is cross-validated in the non-IC group (480 patients), whereas the non-IC model is cross-validated in the IC group (733 patients). Subsequently, C-indices are compared between the IC or non-IC model and the base model.

[a] *p*-value indicating the significance between C-indices is computed using the U-statistic test, mainly with the *rcorrp.cens* function in the *Hmisc* package of R. Abbreviations: C-index, concordance index; CI, confidence interval; IC, induction chemotherapy.

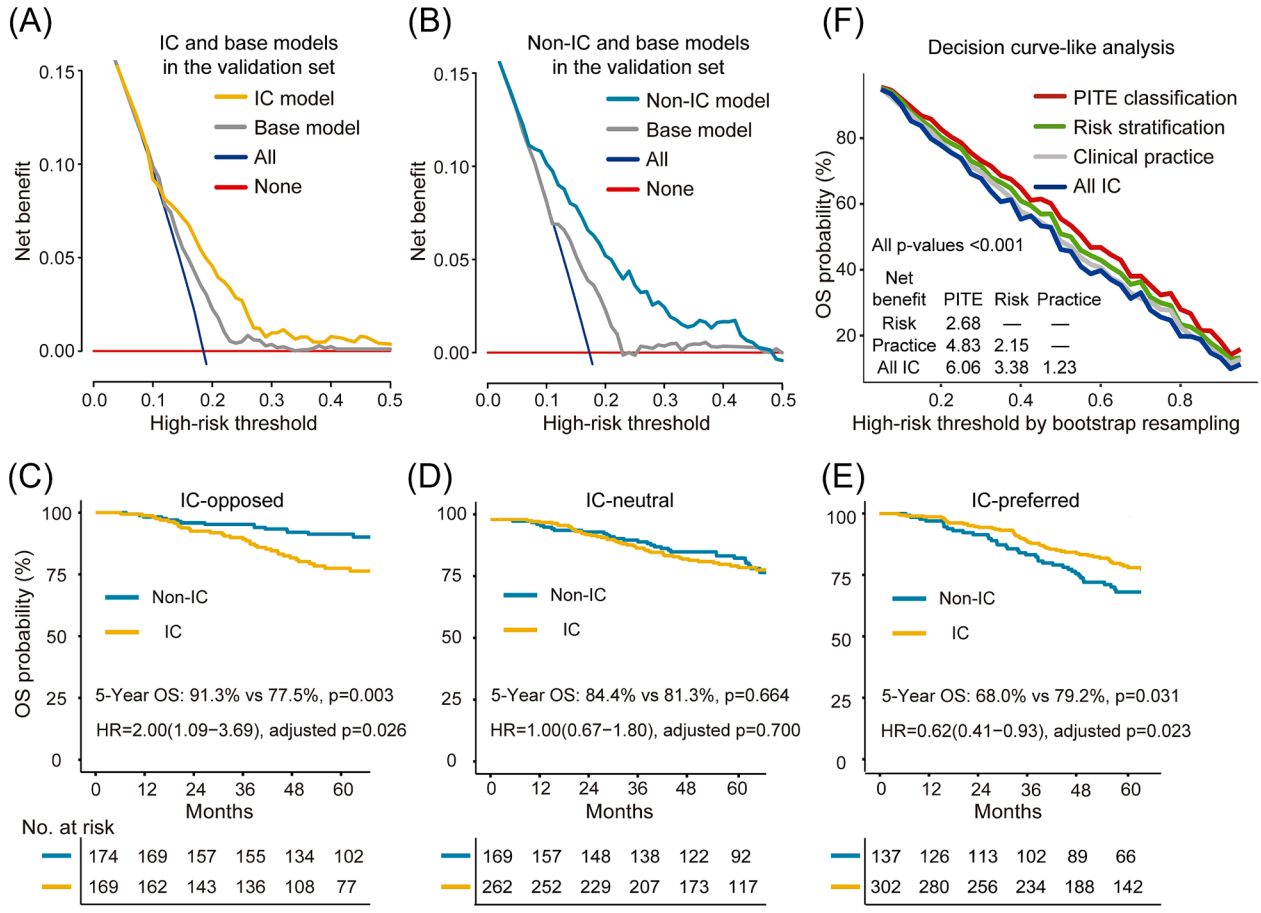

Fig. 3. Decision curves of the prognostic models and validation of ternary PITE classification (**A–B**) Decision curve analysis based on the prognostic models of patients treated with (**A**) IC or (**B**) non-IC regimens in their respective validation sets. (**C–E**) Kaplan–Meier curves of 5-year OS for patients treated with IC or non-IC regimens in the following PITE groups: (**C**) IC-opposed, (**D**) IC-neutral, and **(E)** IC-preferred. (**F**) Decision curve-like analysis for validating the clinical utility of the established PITE classification. In (**F**), the risk stratification is based on the non-IC model, and the inter-pair *p*-values are obtained from a *t*-test. Abbreviations: PITE, predicted individual treatment effect; IC, induction chemotherapy; OS, overall survival; HR, hazard ratio.

as IC-opposed was highest in the T3 stage compared to other T-stages (Supplementary Figure S7). In the IC-opposed group, 52.2 % of patients had slight skull base invasion (Supplementary Table S8).

Finally, the distribution of post-treatment adverse reactions recorded in 917 patients was analyzed, specifically focusing on those within the IC-opposed and IC-neutral groups (Supplementary Table S9). Patients who received IC treatment exhibited significantly higher incidence and severity of adverse reactions compared with those who did not (for example, leukopenia; Fig. 4D). An online application [27] was developed (Supplementary Figure S8) to enhance the clinical applicability of our findings.

Discussion

Here, we successfully established a ternary PITE classification system that accurately categorized individual patients into three groups: IC-preferred, IC-neutral, and IC-opposed. This novel classification closely reflected the real-world clinical scenario, outperforming conventional risk stratification for IC decisions concerning accuracy and net benefit.

In clinical practice, the diverse effects of additional IC on survival can be grouped into three types [15,28,29]: improved, comparable, and reduced. Conventional risk models often produce a binary outcome in which a patient will either benefit or not benefit from IC, which can result in the misclassification of numerous patients who thus would not

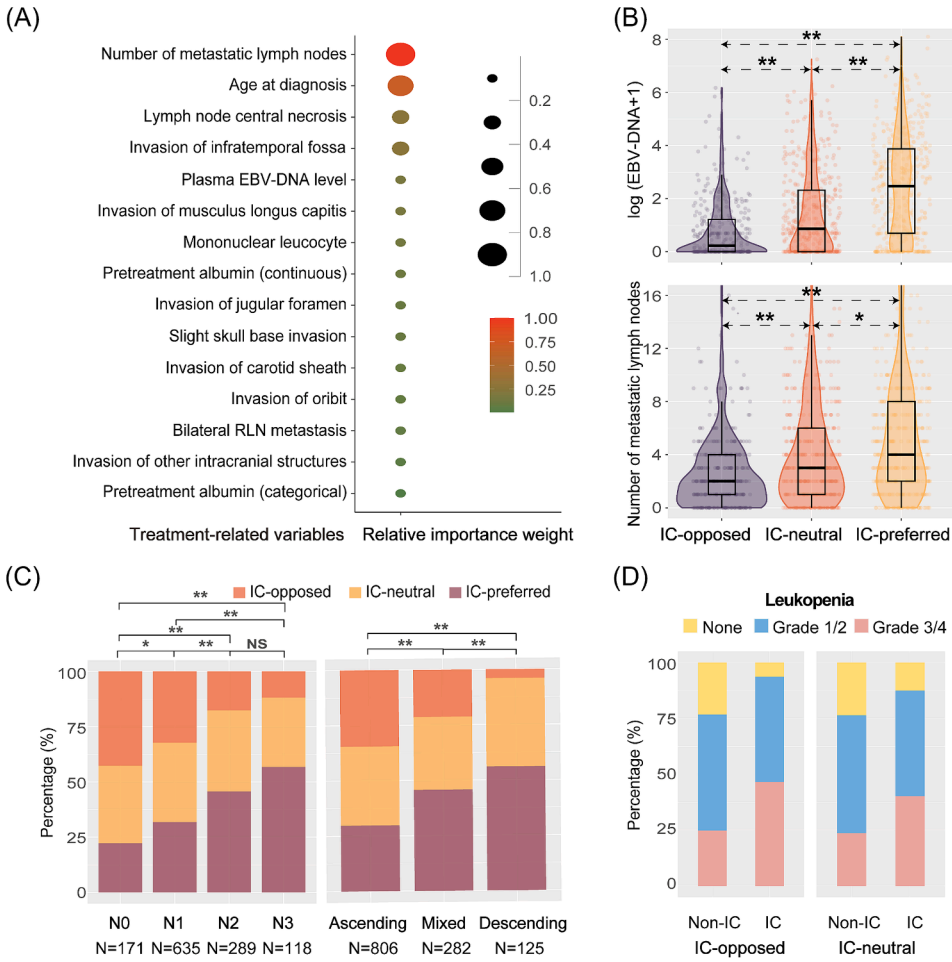

Fig. 4. Distributions of several important variables and adverse reactions (**A**) Relative importance weights of variables in the treatment-related prognostic models. (**B**) Distribution of plasma EBV-DNA level and number of metastatic lymph nodes in PITE groups. (**C**) The distribution of patients, categorized under PITE classification, is analyzed based on their N-stage and NPC extension type. (**D**) Leukopenia is an example of the distribution of adverse reactions in PITE groups (Supplementary Table S9). The intergroup *p*-values are obtained from the Games–Howell post hoc test in (**B**) and the chi-squared test in (**C**). Abbreviations: *p <0.05; **p <0.001; NS, not significant; EBV, Epstein – Barr virus; RLN, retropharyngeal lymph node; IC, induction chemotherapy; PITE, predicted individual treatment effect; NPC, nasopharyngeal carcinoma.

be treated with optimal strategies. We observed that the ternary PITE classification offered an improved method for individualizing IC decisions compared with all three conventional risk stratification methods. It accurately identified patients suitable for IC (IC-preferred group) and those who should avoid it (IC-opposed group). In our study, EBV-DNA level-based stratification failed to identify patients who would benefit from IC. Among high-risk patients classified by the non-IC model, the PITE classification could still accurately identify a significant subset (41.7 %) who would not benefit from IC, yielding a higher OS benefit than risk-based decisions.

The distribution differences between the IC-preferred and combined IC-neutral/opposed groups revealed potential reasons for the unsuitability of IC for this subset of high-risk patients. Specifically, the combined IC-neutral/opposed group had a lower proportion of high plasma EBV-DNA loads and carotid sheath invasions, which are independent negative factors for OS and are associated with IC benefits [26,30,31]. Additionally, this group had a higher proportion of mild/moderate soft-tissue involvement (palatine levator and longus capitis muscles) and slight skull base invasion, which are favorable OS prognosticators and are negatively associated with IC benefits [28,32–34]. The less involvement of T4 stage-related structures indicates less extensive invasion of the primary tumor, suggesting that a less intense treatment approach may be sufficient for this group. These findings highlight that our proposed ternary PITE classification is the nuanced approach for treatment stratification in patients with LANPC.

To provide treatment recommendations, Zhong et al. [19] constructed a nomogram using deep-learning radiomics and pretreatment MR images. They found that, compared with patients treated with CCRT alone, those treated with IC had either superior or inferior disease-free survival, which fell short of recognizing the three distinct types of IC effects. Furthermore, they focused only on patients with T3N1M0-stage disease. Additionally, the interpretability of radiomic features is widely acknowledged. Conversely, our study focused on all patients with LANPC. Our proposed method, integrating features from routinely available structured MRI reports and clinical characteristics, enables a more comprehensive and precise categorization of the heterogeneous effects of IC on tumors, setting a new precedent for the personalization of cancer treatment.

Additional evidence also supported the ternary PITE classification. First, pretreatment plasma EBV-DNA level and number of metastatic lymph nodes are identified as the key predictors in models for PITE. As direct indicators of tumor burden, these biomarkers consistently increased from the IC-opposed to IC-preferred groups, highlighting their role in refining patient stratification for using IC. This aligned with prior research [35,36], and validated our approach. Second, the extension patterns of NPC help categorize LANPC into ascending, descending, and mixed types [37], each with different failure patterns. Given the ability of IC to eliminate micrometastasis early [38], patients with descending

LANPC prone to distant failure can benefit more from IC [20], and consistent results were obtained in our investigation. Third, more than half (52.2 %) of patients in the IC-opposed group had slight skull base invasion, aligning with our previous findings that IC did not improve OS in such cases [28]. Nevertheless, the current staging system classifies such invasion as a T3 characteristic, often leading to the routine but potentially unwarranted use of IC. A recent study suggested that T3 patients with slight skull base invasion should be reclassified as T2 stage [34]. This may explain why, in our study, the proportion of IC-opposed patients was relatively high in the T3 stage. Fourth, the distribution of toxicities within PITE groups met clinical expectations when additional IC was used. Thus, accurate pretreatment identification of the PITE type for each patient could offer substantial clinical value by potentially sparing patients from unnecessary exposure to toxicities related to additional IC.

This study has some limitations. First, the study's retrospective nature in endemic areas suggests that the identified factors for PITE may vary for non-endemic NPC. Second, the study focused on the use of radiological features from structured MRI reports for treatment decision-making in NPC; the influence of diet-related etiological factors was not encompassed in the initial investigation. Third, the PITE classification, built on well-performing and cross-validated prognostic models and validated by subgroup survival analyses, lacks external validation due to the limited sample size. To address this and confirm its clinical robustness, a decision curve-like analysis with 1,000 bootstrap resampling was performed. Finally, prospective trials with larger sample sizes and multiple centers are needed to validate the effectiveness of the PITE classification for NPC and other diseases.

In conclusion, our proposed ternary PITE classification provides a more accurate and clinically beneficial approach to IC decisions than conventional risk stratification does and is promising for refining treatment regimens and reducing unnecessary treatment toxicity. Further external validation and prospective trials are necessary to confirm the utility and generalizability of the ternary PITE classification in clinical practice.

Data availability statement

The raw data were uploaded to the Research Data Deposit public platform (http://www.researchdata.org.cn, RDDA2023440213). The datasets used and/or analyzed during the current study are available from the corresponding authors upon reasonable request.

CRediT authorship contribution statement

Zhiying Liang: Writing – review & editing, Writing – original draft, Methodology, Investigation, Formal analysis. **Chao Luo:** Writing – review & editing, Formal analysis, Data curation. **Shuqi Li:** Methodology, Investigation, Data curation. **Yuliang Zhu:** Writing – review & editing, Software. **Wenjie Huang:** Writing – review & editing, Investigation, Data curation. **Di Cao:** Software, Methodology, Formal analysis. **Yifei Liu:** Investigation, Data curation. **Guangying Ruan:** Resources, Data curation. **Shaobo Liang:** Investigation, Data curation. **Xi Chen:** Writing – review & editing, Investigation. **Kit-Ian Kou:** Validation, Methodology, Conceptualization. **Guoyi Zhang:** Writing – review & editing, Supervision, Project administration. **Lizhi Liu:** Supervision, Resources, Funding acquisition. **Haojiang Li:** Supervision, Software, Methodology, Funding acquisition, Conceptualization.

Funding

This work was supported by the National Natural Science Foundation of China (number 82171906) and the National Natural Science Foundation of China-Regional Science Foundation Project (number 82260358). The funding sources had no role in the study design, collection, analysis and interpretation of data, report's writing; or in the decision to submit the article for publication.

Declaration of competing interest

The authors declare that they have no known competing financial interests or personal relationships that could have appeared to influence the work reported in this paper.

Acknowledgements

We thank Editage (http://www.editage.com) for editing and reviewing English language.

Appendix A. Supplementary material

Supplementary data to this article can be found online at https://doi.org/10.1016/j.radonc.2024.110571.

References

[1] Chien YC, Chen JY, Liu MY, Yang HI, Hsu MM, Chen CJ, et al. Serologic markers of Epstein-Barr virus infection and nasopharyngeal carcinoma in Taiwanese men. N Engl J Med 2001;345:1877–82. https://doi.org/10.1056/NEJMoa011610.
[2] Sung H, Ferlay J, Siegel RL, Laversanne M, Soerjomataram I, Jemal A, et al. Global cancer statistics 2020: GLOBOCAN estimates of incidence and mortality worldwide for 36 cancers in 185 countries. CA Cancer J Clin 2021;71:209–49. https://doi.org/10.3322/caac.21660.
[3] Tang LL, Chen YP, Mao YP, Wang ZX, Guo R, Chen L, et al. Validation of the 8th edition of the UICC/AJCC staging system for nasopharyngeal carcinoma from endemic areas in the intensity-modulated radiotherapy era. J Natl Compr Canc Netw 2017;15:913–9. https://doi.org/10.6004/jnccn.2017.0121.
[4] Lai L, Chen X, Zhang C, Chen X, Chen L, Tian G, et al. Pretreatment plasma EBV-DNA load guides induction chemotherapy followed by concurrent chemoradiotherapy in locoregionally advanced nasopharyngeal cancer: a meta-analysis. Front Oncol 2020;10:610787. https://doi.org/10.3389/fonc.2020.610787.
[5] Guan S, Wei J, Huang L, Wu L. Chemotherapy and chemo-resistance in nasopharyngeal carcinoma. Eur J Med Chem 2020;207:112758. https://doi.org/10.1016/j.ejmech.2020.112758.
[6] NCCN Clinical Practice Guidelines. NCCN clinical practice guidelines in oncology: head and neck cancers, version 3.2024. https://www.nccn.org/professionals/physician_gls/pdf/head-and-neck.pdf; 2024 [Accessed 17 April 2024].
[7] Chen YP, Ismaila N, Chua MLK, Colevas AD, Haddad R, Huang SH, et al. Chemotherapy in combination with radiotherapy for definitive-intent treatment of stage II-IVA nasopharyngeal carcinoma: CSCO and ASCO guideline. J Clin Oncol 2021;39:840–59. https://doi.org/10.1200/JCO.20.03237.
[8] Nazeer F, Poulose JV, Kainickal CT. Induction chemotherapy in nasopharyngeal carcinoma- A systematic review of phase III clinical trials. Cancer Treat Res Commun 2022;32:100589. https://doi.org/10.1016/j.ctarc.2022.100589.
[9] Zhang Y, Chen L, Hu GQ, Zhang N, Zhu XD, Yang KY, et al. Final overall survival analysis of gemcitabine and cisplatin induction chemotherapy in nasopharyngeal carcinoma: a multicenter, randomized phase III trial. J Clin Oncol 2022;40:2420–5. https://doi.org/10.1200/JCO.22.00327.
[10] Liu Y, He S, Wang XL, Peng W, Chen QY, Chi DM, et al. Tumour heterogeneity and intercellular networks of nasopharyngeal carcinoma at single cell resolution. Nat Commun 2021;12:741. https://doi.org/10.1038/s41467-021-21043-4.
[11] Xu C, Chen YP, Liu X, Li WF, Chen L, Mao YP, et al. Establishing and applying nomograms based on the 8th edition of the UICC/AJCC staging system to select patients with nasopharyngeal carcinoma who benefit from induction chemotherapy plus concurrent chemoradiotherapy. Oral Oncol 2017;69:99–107. https://doi.org/10.1016/j.oraloncology.2017.04.015.
[12] Zhang LL, Xu F, Song D, Huang MY, Huang YS, Deng QL, et al. Development of a nomogram model for treatment of nonmetastatic nasopharyngeal carcinoma. JAMA Netw Open 2020;3:e2029882. https://doi.org/10.1001/jamanetworkopen.2020.29882.
[13] Peng H, Dong D, Fang MJ, Li L, Tang LL, Chen L, et al. Prognostic value of deep learning PET/CT-based radiomics: potential role for future individual induction chemotherapy in advanced nasopharyngeal carcinoma. Clin Cancer Res 2019;25:4271–9. https://doi.org/10.1158/1078-0432.CCR-18-3065.
[14] Qiang M, Li C, Sun Y, Sun Y, Ke L, Xie C, et al. A prognostic predictive system based on deep learning for locoregionally advanced nasopharyngeal carcinoma. J Natl Cancer Inst 2021;113:606–15. https://doi.org/10.1093/jnci/djaa149.
[15] Li H, Chen M, Li S, Luo C, Qiu X, Ruan G, et al. Survival impact of additional induction chemotherapy in nasopharyngeal carcinoma with chronic hepatitis B infection: a retrospective, bi-center study. Ann Transl Med 2022;10:731. https://doi.org/10.21037/atm-22-33.
[16] Lin JC, Wang WY, Chen KY, Wei YH, Liang WM, Jan JS, et al. Quantification of plasma Epstein-Barr virus DNA in patients with advanced nasopharyngeal carcinoma. N Engl J Med 2004;350:2461–70. https://doi.org/10.1056/NEJMoa032260.

[17] Qiao H, Tan XR, Li H, Li JY, Chen XZ, Li YQ, et al. Association of intratumoral microbiota with prognosis in patients with nasopharyngeal carcinoma from 2 hospitals in China. JAMA Oncol 2022;8:1301–9. https://doi.org/10.1001/jamaoncol.2022.2810.
[18] Jiang Y, Liang Z, Chen K, Li Y, Yang J, Qu S, et al. A dynamic nomogram combining tumor stage and magnetic resonance imaging features to predict the response to induction chemotherapy in locally advanced nasopharyngeal carcinoma. Eur Radiol 2023;33:2171–84. https://doi.org/10.1007/s00330-022-09201-8.
[19] Zhong L, Dong D, Fang X, Zhang F, Zhang N, Zhang L, et al. A deep learning-based radiomic nomogram for prognosis and treatment decision in advanced nasopharyngeal carcinoma: A multicentre study. EBioMedicine 2021;70:103522. https://doi.org/10.1016/j.ebiom.2021.103522.
[20] Lamont A, Lyons MD, Jaki T, Stuart E, Feaster DJ, Tharmaratnam K, et al. Identification of predicted individual treatment effects in randomized clinical trials. Stat Methods Med Res 2018;27:142–57. https://doi.org/10.1177/0962280215623981.
[21] Kent DM, Steyerberg E, van Klaveren D. Personalized evidence based medicine: predictive approaches to heterogeneous treatment effects. BMJ 2018;363:k4245. https://doi.org/10.1136/bmj.k4245.
[22] Shalit U, Johansson FD, Sontag D. Estimating individual treatment effect: generalization bounds and algorithms. arXiv:1606039762016. https://doi.org/10.48550/arXiv.1606.03976.
[23] Luo C, Li S, Zhao Q, Ou Q, Huang W, Ruan G, et al. RuleFit-based nomogram using inflammatory indicators for predicting survival in nasopharyngeal carcinoma, a Bi-center study. J Inflamm Res 2022;15:4803–15. https://doi.org/10.2147/JIR.S366922.
[24] Wan Y, Tian L, Zhang G, Xin H, Li H, Dong A, et al. The value of detailed MR imaging report of primary tumor and lymph nodes on prognostic nomograms for nasopharyngeal carcinoma after intensity-modulated radiotherapy. Radiother Oncol 2019;131:35–44. https://doi.org/10.1016/j.radonc.2018.11.001.
[25] Yu CN, Greiner R, Lin HC, Baracos VE. In: Learning patient-specific cancer survival distributions as a sequence of dependent regressors. Granada, Spain: Curran Associates Inc; 2011. p. 1845–53.
[26] Tang LQ, Li CF, Li J, Chen WH, Chen QY, Yuan LX, et al. Establishment and validation of prognostic nomograms for endemic nasopharyngeal carcinoma. J Natl Cancer Inst 2016;108:djv291. https://doi.org/10.1093/jnci/djv291.
[27] Predicted Individual Treatment Effect of Induction Chemotherapy for Nasopharyngeal Carcinoma. https://npc2ite.shinyapps.io/shinyite/; 2024 [Accessed 17 April 2024].
[28] Li S, Luo C, Huang W, Zhu S, Ruan G, Liu L, et al. Value of skull base invasion subclassification in nasopharyngeal carcinoma: implication for prognostic stratification and use of induction chemotherapy. Eur Radiol 2022;32:7767–77. https://doi.org/10.1007/s00330-022-08864-7.
[29] Dahabreh IJ, Hayward R, Kent DM. Using group data to treat individuals: understanding heterogeneous treatment effects in the age of precision medicine and patient-centred evidence. Int J Epidemiol 2016;45:2184–93. https://doi.org/10.1093/ije/dyw125.
[30] Liu L-T, Tang L-Q, Chen Q-Y, Zhang L, Guo S-S, Guo L, et al. The prognostic value of plasma epstein-barr viral DNA and tumor response to neoadjuvant chemotherapy in advanced-stage nasopharyngeal carcinoma. Int J Radiat Oncol Biol Phys 2015;93:862–9. https://doi.org/10.1016/j.ijrobp.2015.08.003.
[31] Quan T, Guan W, Huang W, Cui C, Li H, Ruan G, et al. Carotid space involvement is a prognostic factor and marker for induction chemotherapy in patients with nasopharyngeal carcinoma. Oral Oncol 2022;135:106230. https://doi.org/10.1016/j.oraloncology.2022.106230.
[32] Dong A, Huang W, Ma H, Cui C, Zhou J, Ruan G, et al. Grading soft tissue involvement in nasopharyngeal carcinoma using network and survival analyses: a two-center retrospective study. J Magnetic Resonance Imaging : JMRI 2021;53:1752–63. https://doi.org/10.1002/jmri.27515.
[33] Li H-J, Hu Y-Y, Huang L, Zhou J, Li J-J, Xie C-B, et al. Subclassification of skull-base invasion for nasopharyngeal carcinoma using cluster, network and survival analyses: A double-center retrospective investigation. Radiother Oncol: J Eur Soc Therap Radiol Oncol 2019;134:37–43. https://doi.org/10.1016/j.radonc.2019.01.021.
[34] Du X-J, Wang G-Y, Zhu X-D, Han Y-Q, Lei F, Shen L-F, et al. Refining the 8th edition TNM classification for EBV related nasopharyngeal carcinoma. Cancer Cell 2024;42. https://doi.org/10.1016/j.ccell.2023.12.020.
[35] Xu C, Zhang S, Li WF, Chen L, Mao YP, Guo Y, et al. Selection and validation of induction chemotherapy beneficiaries among patients with T3N0, T3N1, T4N0 nasopharyngeal carcinoma using epstein-barr virus DNA: a joint analysis of real-world and clinical trial data. Front Oncol 2019;9:1343. https://doi.org/10.3389/fonc.2019.01343.
[36] Zhao Q, Dong A, Cui C, Ou Q, Ruan G, Zhou J, et al. MRI-based metastatic nodal number and associated nomogram improve stratification of nasopharyngeal carcinoma patients: potential indications for individual induction chemotherapy. J Magn Reson Imaging 2023;57:1790–802. https://doi.org/10.1002/jmri.28435.
[37] Yao JJ, Qi ZY, Liu ZG, Jiang GM, Xu XW, Chen SY, et al. Clinical features and survival outcomes between ascending and descending types of nasopharyngeal carcinoma in the intensity-modulated radiotherapy era: a big-data intelligence platform-based analysis. Radiother Oncol 2019;137:137–44. https://doi.org/10.1016/j.radonc.2019.04.025.
[38] Tan TH, Soon YY, Cheo T, Ho F, Wong LC, Tey J, et al. Induction chemotherapy for locally advanced nasopharyngeal carcinoma treated with concurrent chemoradiation: a systematic review and meta-analysis. Radiother Oncol 2018;129:10–7. https://doi.org/10.1016/j.radonc.2018.02.027.